



# Assessment of Radial basis function based meshfree method for the buckling analysis of rectangular FGM plate using HSDT and Strong form formulation

Rahul Kumar <sup>a\*</sup>, Mukesh Singh <sup>b</sup>, Chandan Kumar <sup>c</sup>, Jay Damania <sup>a</sup>, Jigyasa Singh <sup>d</sup>, Jeeoot Singh <sup>d</sup>

<sup>a</sup> Department of Mechanical Engineering, Sardar Vallabhbhai National Institute of Technology, Surat-395007, India

<sup>b</sup> Department of Mechanical Engineering, BIT Mesra, off campus, Patna-80014, India

<sup>c</sup> Institute of Business Management, GLA University, Mathura- 281406, India

<sup>d</sup> Department of Mechanical Engineering, MMMUT, Gorakhpur-273010, India

## Abstract

An effort has been made in modifying the radial distances of existing radial basis functions (RBFs) for the buckling analysis of functionally graded material (FGM) rectangular plates. The governing differential equations (GDE's) and boundary conditions are developed by employing the energy principle. The novelty of the present modified RBFs is that they are suitable for analyzing plates with varying aspect ratios. In the present analysis, thirteen different RBFs available in the literature are analyzed. It is found that all RBFs are well suited for buckling analysis of FGM plates with a different aspect ratio which was not possible with existing RBFs. Existing RBFs were suitable for analyzing square plates. To demonstrate the accuracy and efficiency of the present method, results are obtained for the buckling load parameters with modified radial distances for different aspect ratios. The results of several numerical examples have shown that the present modified RBF-based meshfree methods are well suited and accurate for analyzing rectangular plates. The effect of aspect ratio with grading index, span to thickness ratio on the normalized critical buckling load is discussed.

**Keywords:** Rectangular plate; FGM; RBF; Meshfree; Buckling

## 1. INTRODUCTION

Radial basis function (RBF) based meshfree methods are effective techniques that have been widely implemented for multivariate data fitting over scattered data. This method is mainly applied to solve higher order partial differential equation problems with high convergence order numerically. Therefore, RBF-based meshfree methods have attracted many researchers in the recent past. The RBF method proposed as a multi quadric method was firstly implemented by Hardy [1] in 1971, and after almost two decades, Kansa [2, 3] has implemented the multiquadric radial basis function (MQ-RBF) method to solve various kinds of partial differential equations (PDEs). Many researchers and scientists have found the optimal shape parameter utilized in the MQ-RBF[4-8]. Fasshauer [9] explored a relation between multigrid finite elements and multilevel RBF with smoothing. Wendland[10] combined the RBFs with the field of Galerkin methods to solve PDEs. Farahani et al. [11] explained the optimal shape parameter of Wendland's RBF for

\* Corresponding author. Tel.: +917543934007.

E-mail address: rahul22mech@gmail.com

bending analysis of plates. Ferreira et al. [12-20] utilized the RBFs based meshless method for the analysis of plates and shells. Xiang et al.[21-25] utilized inverse multiquadric, Gaussian, and thin-plate spline RBFs based meshless method for the analysis of plates. Rodrigues et al.[26] implemented the RBFs -finite differences technique for the structural analysis of laminated plates. Roque et al.[27] used the RBF-Finite differences collocation method for the analysis of composite plates. Jeeoot [28-38] used RBF based meshless method for the analysis of square plates. Kumar et al. [39-47] used different types of RBFs for the analysis of FGM plates. Neves et al.,[48-50] used the RBF method to analyse FGM plates and shells. Maturi et al. [51] investigated static and free vibration analysis of sandwich plates by using the RBF technique.

Recently, many researchers have done various studies on the buckling and vibration analysis of plates in order to use it effectively and efficiently but buckling analysis by meshfree methods is available very few.

Thai et al.[52] investigated static, dynamic, and buckling analysis of FGM and sandwich plate by using modified Moving Kriging (MK) interpolation-based meshfree method. Bui et al.[53] investigate buckling analysis using the meshfree method under uniformly uniaxial, biaxial, and pure shear loads. Rodrigues et al.[54] investigated bending, vibration, and buckling analysis of laminated plates based on RBFs-differential quadrature collocation. Chu et al. [55] used the Hermite radial basis function collocation method for the buckling analysis of the FGM plate.. Many research work[56-62] carried out for the buckling analysis of plate and shells via nonlocal elasticity theory. Liew et al.[63] used meshfree method for buckling and vibration analysis of plates based on FSDT formulation. Zhang et al. [64] implemented Kriging meshless method for thermal buckling of FGM plates. Tan et al. [65] used an Isogeometric-meshfree technique for the analysis of 3D FGM plates and shells. Zarei and Khosravifard [66] investigated static and buckling analysis using the meshfree technique. The numerous papers published to offer the detailed study on vibration of plates, shell, and structure [56-59, 61, 67-105] . Hosseini et al. [106] investigated the effect of various parameters on the stress analysis of rotating nano-disk made of FGMs. Nejad et al. [107] studied the static analysis of the BDFG nano-beam via the Rayleigh-Ritz method. Khoram et al. [108] used the Eringen's nonlocal elasticity theory to study the mechanical behaviour of the nanobeam. Do et al. [109] investigated thermal buckling of FGM plate by using improved radial point interpolation function. Asemi et. al [110] examined the post-buckling analysis of orthotropic single-layered graphene sheet applying the nonlocal theory via Galerkin method. Hadi et al. [111] utilized the energy method and stress analysis to investigate the stresses and strains of a FGM beam subjected to an arbitrary transvers loading. Farajpour et. al [94] proposed a new explicit formula for the length-dependent persistence length of microtubules with consideration of surface effects. Farajpour et. al [103] proposed a new size-dependent plate model based on the higher-order nonlocal strain gradient theory for the buckling of nanoplates. Mohammadi et. al [98] studied the free vibration behaviour of rectangular graphene sheet under shear in-plane load by applying nonlocal elasticity theory. Mohammadi et. al [92] investigated the effect of the temperature change on the vibration frequency of elastically supported mono-layer graphene sheet via nonlocal elasticity theory.

To the best of authors' knowledge, few efforts of researchers have been paid on the performance of RBF-based meshfree method in investing FGM rectangular plate. Up to now, there does not exist a proper way to investigate the rectangular plate without changing the shape parameters, and it is still an important issue in the RBFs based meshfree method to determine the rectangular plate without changing shape parameters. The present study addresses, for the first time, a five variable HSDT for buckling analysis of FGM rectangular plate by using thirteen MRBFs based meshfree method. The newly proposed expression for MRBFs is implemented and successfully applied for the analysis of rectangular FGM plates.

## 2 MATHEMATICAL FORMULATIONS

Consider rectangular FGM plate with dimensions  $(a \times b \times h)$  in the cartesian coordinate system  $(x-y-z)$ . The mid-plane of the plate is considered the reference plane. The displacement field  $u$ ,  $v$ , and  $w$  at any point along the  $x$ -,  $y$ - and  $z$ -axes can be expressed as in terms of the mid-plane displacements  $u_0$ ,  $v_0$ ,  $w_0$  and rotations  $\phi_x$  and  $\phi_y$ .

$$\begin{aligned} u &= u_0(x, y) - z \frac{\partial w_0(x, y)}{\partial x} + f(z)\phi_x(x, y) \\ v &= v_0(x, y) - z \frac{\partial w_0(x, y)}{\partial y} + f(z)\phi_y(x, y) \\ w &= w_0(x, y) \end{aligned} \quad (1)$$

Where,  $f(z) = p \left( \left( \frac{z}{h} \right)^3 - \frac{3}{4h} z \right)$  is transverse shear function.

The volume fraction of the metal phase is obtained by.

$$V_m(z)=1-V_c(z) \tag{2}$$

The material property variation along the plate thickness is given by the following relations,

$$E(z)=[E_c - E_m] \left(\frac{2z+h}{2h}\right)^n + E_m \tag{3}$$

$$\rho(z)=[\rho_c - \rho_m] \left(\frac{2z+h}{2h}\right)^n + \rho_m \tag{4}$$

In the above equations, the young’s moduli of the metallic and ceramic constituents are given by  $E_m$  and  $E_c$  respectively. The material properties vary according to the power-law distribution where ‘n’ represents the grading index.

Strain-displacement relations are expressed as:

$$\left\{ \begin{matrix} \epsilon_{xx} \\ \epsilon_{yy} \\ \gamma_{xy} \end{matrix} \right\} = \left\{ \begin{matrix} \frac{\partial u}{\partial x} \\ \frac{\partial v}{\partial y} \\ \frac{\partial u}{\partial y} + \frac{\partial v}{\partial x} \end{matrix} \right\} = \left\{ \begin{matrix} \frac{\partial u_0}{\partial x} - z \frac{\partial^2 w_0}{\partial x^2} + f(z) \frac{\partial \phi_x}{\partial x} \\ \frac{\partial v_0}{\partial y} - z \frac{\partial^2 w_0}{\partial y^2} + f(z) \frac{\partial \phi_y}{\partial y} \\ \frac{\partial u_0}{\partial y} + \frac{\partial v_0}{\partial x} - 2z \frac{\partial^2 w_0}{\partial x \partial y} + f(z) \frac{\partial \phi_x}{\partial y} + f(z) \frac{\partial \phi_y}{\partial x} \end{matrix} \right\} \tag{5}$$

And,

$$\left\{ \begin{matrix} \gamma_{yz} \\ \gamma_{zx} \end{matrix} \right\} = \left\{ \begin{matrix} \frac{\partial v}{\partial z} + \frac{\partial w}{\partial y} \\ \frac{\partial u}{\partial z} + \frac{\partial w}{\partial x} \end{matrix} \right\} = \left\{ \begin{matrix} \frac{\partial f(z)}{\partial z} \phi_y \\ \frac{\partial f(z)}{\partial z} \phi_x \end{matrix} \right\} \tag{6}$$

The stress-strain relation using Hook’s law with respect to the structural axis system (X-Y-Z) for the FGM plate may be expressed as :

$$\left\{ \begin{matrix} \sigma_{xx} \\ \sigma_{yy} \\ \sigma_{xy} \\ \sigma_{yz} \\ \sigma_{zx} \end{matrix} \right\} = \left[ \begin{matrix} \bar{Q}_{11} & \bar{Q}_{12} & 0 & 0 & 0 \\ \bar{Q}_{12} & \bar{Q}_{22} & 0 & 0 & 0 \\ 0 & 0 & \bar{Q}_{66} & 0 & 0 \\ 0 & 0 & 0 & \bar{Q}_{44} & 0 \\ 0 & 0 & 0 & 0 & \bar{Q}_{55} \end{matrix} \right] \left\{ \begin{matrix} \epsilon_{xx} \\ \epsilon_{yy} \\ \gamma_{xy} \\ \gamma_{yz} \\ \gamma_{zx} \end{matrix} \right\} \tag{7}$$

Where,

$$\bar{Q}_{11} = \bar{Q}_{22} = \frac{E}{(1-\nu^2)}, \quad \bar{Q}_{12} = \frac{\nu E}{(1-\nu^2)}, \quad \bar{Q}_{44} = \bar{Q}_{55} = \bar{Q}_{66} = G = \frac{E}{2(1+\nu)}$$

The GDEs of the plate are obtained using energy principle and expressed as:

$$\delta u_0 : \frac{\partial N_{xx}}{\partial x} + \frac{\partial N_{xy}}{\partial y} = 0 \tag{8}$$

$$\delta v_0 : \frac{\partial N_{xy}}{\partial x} + \frac{\partial N_{yy}}{\partial y} = 0 \tag{9}$$

$$\delta w_0: \frac{\partial^2 M_{xx}}{\partial x^2} + \frac{\partial^2 M_{yy}}{\partial y^2} + 2 \frac{\partial^2 M_{xy}}{\partial x \partial y} = N_{xx}^b \frac{\partial^2 w}{\partial x^2} + N_{yy}^b \frac{\partial^2 w}{\partial y^2} + 2 N_{xy}^b \frac{\partial^2 w}{\partial x \partial y} \tag{10}$$

$$\delta \phi_x: \frac{\partial M_{xx}^f}{\partial x} + \frac{\partial M_{xy}^f}{\partial y} - Q_x^f = 0 \tag{11}$$

$$\delta \phi_y: \frac{\partial M_{xy}^f}{\partial x} + \frac{\partial M_{yy}^f}{\partial y} - Q_y^f = 0 \tag{12}$$

Where,  $N_{xx}^b, N_{yy}^b$  are the in-plane forces and  $N_{xy}^b$  is the in-plane shear force. The force and moment resultants in the plate are expressed as:

$$N_{ij}, M_{ij}, M_{ij}^f = \int_{-h/2}^{+h/2} (\sigma_{ij}, z\sigma_{ij}, f(z)\sigma_{ij}) dz \tag{13}$$

$$Q_x^f, Q_y^f = \int_{-h/2}^{+h/2} (\sigma_{xz}, \sigma_{yz}) \left( \frac{\partial f(z)}{\partial z} \right) dz \tag{14}$$

Boundary condition for simply supported plate is expressed as

$$\begin{aligned} x = 0, a: N_{xx} = 0, v_0 = 0, w_0 = 0, M_{xx} = 0, \phi_y = 0 \\ y = 0, b: u_0 = 0, N_{yy} = 0, w_0 = 0, \phi_x = 0, M_{yy} = 0 \end{aligned} \tag{15}$$

### 3 SOLUTION METHODOLOGY

RBF-based meshfree method is one of the best and most powerful approaches to solve the system of PDEs with higher accuracy. The significant feature of the RBF-based meshfree method is that it does not require meshes. However, the method accuracy and stability are extremely dependent on an appropriate choice of a shape parameter ‘k.’ The modification of radial distance between the nodes for rectangular coordinates is done in such a way that the aspect ratio starts changing without changing the shape parameters. The expression used for square plate

$$r = \|X - X_j\| = \sqrt{(x - x_j)^2 + (y - y_j)^2} \text{ has been modified as } r = \|X - X_j\| = \sqrt{\left(\frac{x - x_j}{a}\right)^2 + \left(\frac{y - y_j}{b}\right)^2} \text{ for rectangular plate}$$

where a and b are the length and breadth of a rectangular plate. And various types of RBFs used in computational applications are listed in Table 1. The considered GDEs with five unknown variables  $u_0, v_0, w_0, \phi_x$  and  $\phi_y$  can be interpolated in the form of the modified radial distance between nodes. To eliminate the singularity, an infinitesimally small value is added for zero radial distance. All computational calculations are carried out in MATLAB with a 2.7 GHz Corei7 processor.

**Table 1: Various types of RBFs used in computation applications.**

S. No	RBFs
1	Polynomial, $g1 = r^k$
2	Gaussian quadratic, $g2 = e^{(-k^2 r^2)}$
3	Thin Plate Spline, $g3 = \log(r) r^{2k}$
4	Wendland’s C2, $g4 = (1 - kr)^4 (4kr + 1)$
5	Wendland’s C4, $g5 = (1 - kr)^6 \left( (35(kr)^2) + (18kr) + 3 \right)$
6	Wendland’s C6, $g6 = (1 - kr)^8 \left( (32(kr)^3) + (25(kr)^2) + (8kr) + 1 \right)$
7	Hyperbolic secant, $g7 = \text{sech}(k\sqrt{r})$
8	Wu-C2, $g8 = (1 - kr)^5 \left( 8 + 40kr + 48(kr)^2 + 25(kr)^3 + 5(kr)^4 \right)$

9	$Wu-C4, g9 = (1 - kr)^6 (6 + 36kr + 82(kr)^2 + 72(kr)^3 + 30(kr)^4 + 5(kr)^5)$
10	Hardy's Multiquadric, $g10 = \sqrt{(k^2 + r^2)}$
11	Hardy's Inverse Quadric $g11 = (k^2 + r^2)^{-1}$
12	Inverse Multi-quadric, $g12 = (\sqrt{1 + (kr)^2})^{-1}$
13	Generalized Inverse Multi-quadric, $g13 = (1 + (kr)^2)^{-2}$

The convergence of results was checked by shifting the shape parameter. When convergence is confirmed and stable, the accuracy is likewise checked. Also, in view of stability and accuracy, the authors calculate the shape parameter. The discretization of GDEs for five unknown variables is considered by. The value of 'p' is also optimized for accuracy, and it is found that 'p=0.9' is a better choice.

### 4 RESULTS AND DISCUSSION

In this section, various numerical examples are presented and discussed to verify the convergence and accuracy of the present theory and RBFs for predicting the buckling analysis of simply supported FGM plates. The material properties of FGM used in computing results are  $E_c=360$  GPa,  $E_m=70$  GPa,  $\nu=0.3$ .

#### 4.1 Convergence study

The first example is performed for the convergence study of the rectangular FGM plate. The obtained results by thirteen RBFs are compared with 2-D HSDT via Navier-type analytical solutions [112] and quasi-3D via Navier solution.[113] The aspect ratio is taken as 0.5 with grading index=2. From Table 2, it is observed that all the results obtained by modifying RBFs are in good agreement with the 2-D HSDT and 3-D HSDT result of rectangular FGM plate under uniaxial load. In 15x15 nodes, the convergence rate % is less than 1% for all the RBFs. So, 15x15 nodes are considered throughout the study.

#### 4.2 Comparison study

To check the accuracy and effectiveness of the present methodology, various comparison study has been done for the buckling analysis of the FGM plate. Table 3 shows the comparison study of an isotropic rectangular plate with the 3D result via differential quadrature [114] under biaxial load. The span to thickness ratio is 10. When the thirteen RBFs are compared to 3D results via differential quadrature [114], it can be observed that as the aspect ratio increase from 1 to 2, the diff % decreases for all the RBFs. All the RBFs are in good agreement with the 3D result via differential quadrature result in the literature.

**Table 1: Convergence and validation study of normalized buckling  $\bar{N}_{cr} = N_{cr} a^2 / E_m h^3$  of rectangular FGM plate under uniaxial load ( $a/b=0.5, n=2, a/h=20$ )**

RBFs	Number of nodes						Ref. [112]	Ref. [113]
	11x11	12x12	13x13	14x14	15x15	16x16		
g1	2.9722	2.9757	2.9790	2.9710	2.9711	2.9730	2.9585	3.0968
g2	2.8808	2.9321	2.9296	2.9258	2.9106	2.9297	2.9585	3.0968
g3	2.9316	2.9504	2.9515	2.9548	2.9558	2.9567	2.9585	3.0968
g4	2.9722	2.9757	2.9790	2.9710	2.9711	2.9730	2.9585	3.0968
g5	2.9683	2.9655	2.9641	2.9261	2.9614	2.9612	2.9585	3.0968
g6	2.9521	2.9572	2.9564	2.9575	2.9575	2.9578	2.9585	3.0968
g7	3.0000	2.9692	2.9498	2.9498	2.9584	2.9625	2.9585	3.0968
g8	2.9400	2.9453	2.9521	2.9537	2.9555	2.9562	2.9585	3.0968
g9	2.9522	2.9572	2.9564	2.9575	2.9575	2.9578	2.9585	3.0968

g10	2.9249	2.9374	2.9283	2.9354	2.9330	2.9362	2.9585	3.0968
g11	2.9865	2.9816	2.9721	2.9715	2.9653	2.9661	2.9585	3.0968
g12	3.0133	3.0041	2.9782	2.9748	2.9657	2.9640	2.9585	3.0968
g13	3.0096	3.0151	2.9700	2.9788	2.9626	2.9660	2.9585	3.0968

**Table 2: Comparison study for normalized buckling of rectangular isotropic plate under biaxial load.**

Method	Aspect ratio, b/a					*Avg diff %
	1	1.25	1.5	1.75	2	
Ref. [114]	1.871	1.552	1.376	1.268	1.198	
g1	1.893	1.567	1.387	1.277	1.206	-0.86
g2	1.893	1.566	1.384	1.273	1.200	-0.64
g3	1.895	1.569	1.389	1.279	1.208	-1.01
g4	1.893	1.567	1.387	1.277	1.206	-0.86
g5	1.895	1.569	1.390	1.280	1.209	-1.05
g6	1.891	1.566	1.387	1.278	1.206	-0.85
g7	1.894	1.572	1.387	1.279	1.208	-1.00
g8	1.891	1.566	1.387	1.278	1.206	-0.85
g9	1.894	1.568	1.388	1.279	1.208	-0.97
g10	1.907	1.572	1.387	1.275	1.202	-0.98
g11	1.897	1.571	1.391	1.281	1.209	-1.13
g12	1.897	1.571	1.391	1.281	1.21	-1.15
g13	1.898	1.57	1.39	1.28	1.208	-1.08

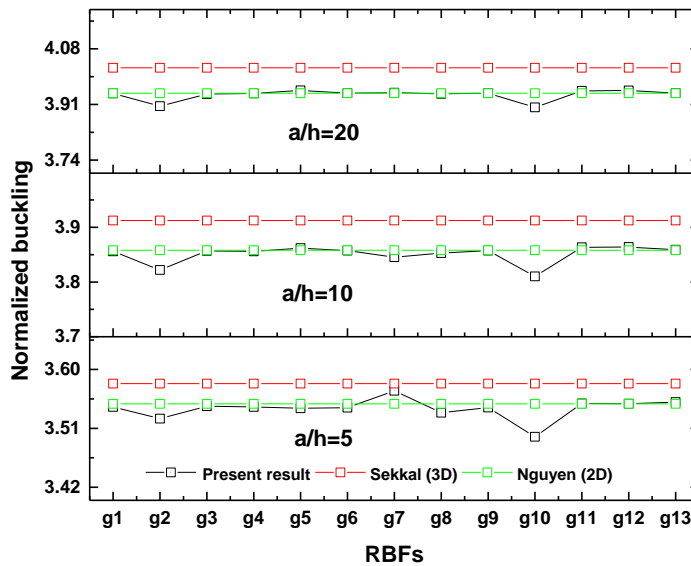
\*Where Avg. Diff %= Abs ((Ref. results -Present result-)/ Ref. result) x100

**Table 4: Comparison Study of normalized buckling  $\bar{N}_{cr} = N_{cr}a^2 / E_m h^3$  of rectangular FGM plate under uniaxial load. ( $a/b=0.5$ ,  $a/h=10$ )**

Methods	Grading Index						Average diff% Ref [112]	Average diff% Ref [113]
	0	0.5	1	2	5	10		
Ref. [112]	7.4126	4.8904	3.8221	3.0168	2.509	2.2374	-	-
Ref [113]	7.4115	4.8225	3.7137	2.8911	2.4155	2.1911	-	2.37
g1	7.3935	4.8200	3.7187	2.9026	2.4256	2.1929	-0.12	2.25
g2	7.3586	4.7768	3.6659	2.8474	2.3847	2.1673	1.14	3.47
g3	7.4079	4.8213	3.7110	2.8892	2.4168	2.1906	0.03	2.40
g4	7.3935	4.8200	3.7187	2.9026	2.4256	2.1929	-0.12	2.25
g5	7.4159	4.8272	3.7164	2.8922	2.4185	2.1918	-0.07	2.30
g6	7.4078	4.8218	3.7117	2.8900	2.4170	2.1904	0.02	2.39
g7	7.4037	4.8182	3.7144	2.8879	2.4160	2.1816	0.12	2.48
g8	7.3984	4.8161	3.7074	2.8866	2.4138	2.1872	0.15	2.51
g9	7.4078	4.8218	3.7117	2.8900	2.4170	2.1904	0.02	2.39
g10	7.3121	4.7634	3.6709	2.8612	2.3911	2.1645	1.16	3.50
g11	7.4170	4.8293	3.7191	2.8972	2.4226	2.1944	-0.17	2.20
g12	7.4181	4.8300	3.7196	2.8974	2.4227	2.1945	-0.18	2.19
g13	7.4075	4.8235	3.7159	2.8959	2.4217	2.1930	-0.09	2.28

Where Avg. Diff %= Abs ((Ref. results -Present result-)/ Ref. result) x100

Table 4 shows the effect of grading index and RBFs on normalized buckling of FGM plate under uniaxial load. Aspect ratio is taken as 0.5 with a span to thickness ratio is 10. The RBFs results are compared with the 2-D HSDT [112], and 3-D HSDT [113] result in the literature. It can be observed that RBFs g1, g4, g5, g11, g12 and g13 predict a good result as compared to 2-D HSDT [112]. g1 and g10 predict higher average diff %. It can also be seen that normalized buckling decrease by increasing the value of the grading index.



It can also be seen that normalized buckling decrease by increasing the value of the grading index.

**Fig 1: Comparison study for RBFs with span to thickness ratio on normalized buckling  $\bar{N}_{cr} = N_{cr} a^2 / E_m h^3$  of FGM plate under biaxial load.**

Figure 1 presents the variation of normalized buckling in terms of RBFs and span to thickness ratio. Aspect ratio is taken as 0.5 and grading index is 0.5. It can be noticed that g2 and g10 under predict with 2-D HSDT via Navier-type analytical solutions and quasi-3D via Navier solution for all span to thickness ratio. g11, g12 and g13, over predicts the HSDT and under predict with the quasi-3D z results. Overall, the present methodology is good for analysing the rectangular plate. It can also be observed that by increasing the span to thickness ratio, normalized buckling also increased.

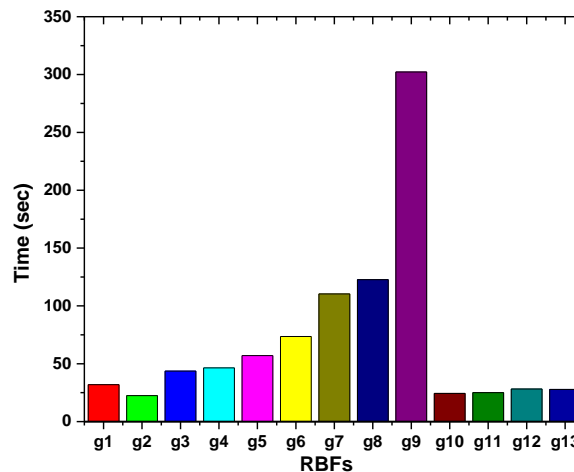


**Fig 2: Comparison study of RBFs with computational speed**

Now the comparison study of all RBFs with the time taken to compute the buckling results. From Figure 2, it can

be observed that g2, g10, g11, g12, and g13 take less computational time as compared to other RBFs and g9 takes maximum time.

### 4.3 Parametric study

#### 4.3.1 Effect of grading index with an aspect ratio

In this section, the effect of aspect ratio on normalized buckling of FGM plate ( $a/h=10$ , g11) under biaxial loading is investigated and presented in Table 5. It is observed that by increasing the grading index for all aspect ratio and modes, normalized buckling decreases. It is also noticed that normalized buckling also increases by increasing the aspect ratio. Figure 3 represents the effect of grading index on normalized buckling of FGM plate under uniaxial loading ( $a/b=0.5,1$ ). It is noticed that by increasing the grading index for  $a/b=0.5$  and  $a/b=1$ , the normalized buckling decreases, and after  $n=5$ , the effect of the grading index is constant.

**Table 5: Effect of aspect ratio on normalized buckling  $\bar{N}_{cr} = N_{cr} a^2 / E_m h^3$  of FGM plate under biaxial loading.**

a/b	Modes	0	1	2	3	5	10
0.5	1	5.934	2.975	2.318	2.101	1.938	1.756
	2	9.306	4.680	3.641	3.292	3.025	2.733
	3	14.614	7.386	5.734	5.166	4.718	4.242
	4	18.668	9.472	7.345	6.598	5.996	5.372
1	1	9.309	4.681	3.642	3.293	3.026	2.733
	2	21.556	10.965	8.492	7.614	6.897	6.165
	3	21.556	10.965	8.492	7.614	6.897	6.165
	4	32.139	16.509	12.738	11.336	10.145	8.993
1.5	1	14.640	7.399	5.745	5.177	4.727	4.250
	2	26.141	13.351	10.323	9.226	8.314	7.406
	3	38.381	19.833	15.266	13.527	12.020	10.602
	4	41.945	21.745	16.713	14.771	13.074	11.501
2	1	21.5586	10.965	8.494	7.617	6.900	6.169
	2	32.129	16.499	12.729	11.331	10.143	8.993
	3	46.771	24.351	18.685	16.460	14.495	12.706
	4	56.590	29.748	22.743	19.898	17.332	15.082
2.5	1	29.636	15.186	11.730	10.460	9.391	8.341
	2	39.178	20.248	15.583	13.805	12.263	10.814
	3	52.514	27.482	21.044	18.469	16.166	14.114
	4	67.136	35.632	27.132	23.567	20.305	17.541
3	1	38.447	19.862	15.293	13.556	12.052	10.633
	2	46.940	24.432	18.752	16.526	14.559	12.766
	3	58.918	31.011	23.694	20.707	18.008	15.653
	4	72.204	38.493	29.262	25.335	21.722	18.705



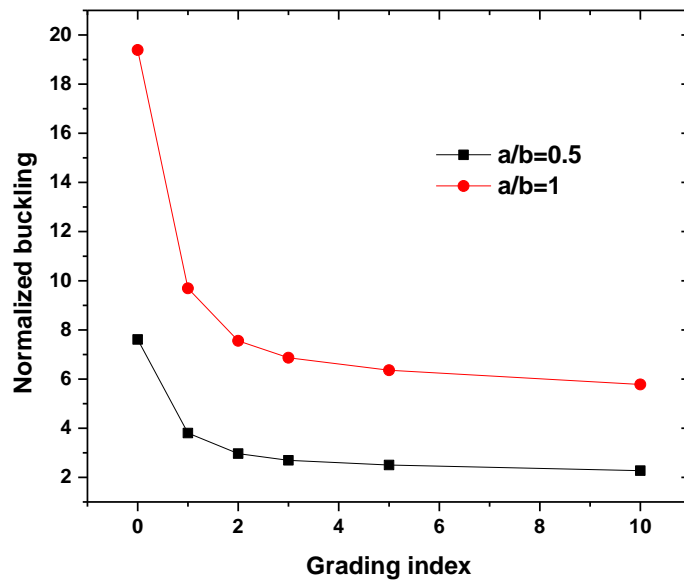


Fig 3: The effect of grading index on normalized buckling  $\bar{N}_{cr} = N_{cr} a^2 / E_m h^3$  of FGM plate under uniaxial loading.

4.3.2 Effect of span to thickness ratio with an aspect ratio

Now, the effect of span to thickness ratio with different aspect ratios for normalized buckling of FGM plate (n=2, g 12) under biaxial loading is investigated and shown in Figure 4. It is observed that all the aspect ratio shows the same nature, and by increasing the span to thickness ratio, normalized buckling also increases, and after a/h=50, the influences of a/h is constant. It is also noted that normalized buckling increases by increasing the aspect ratio.

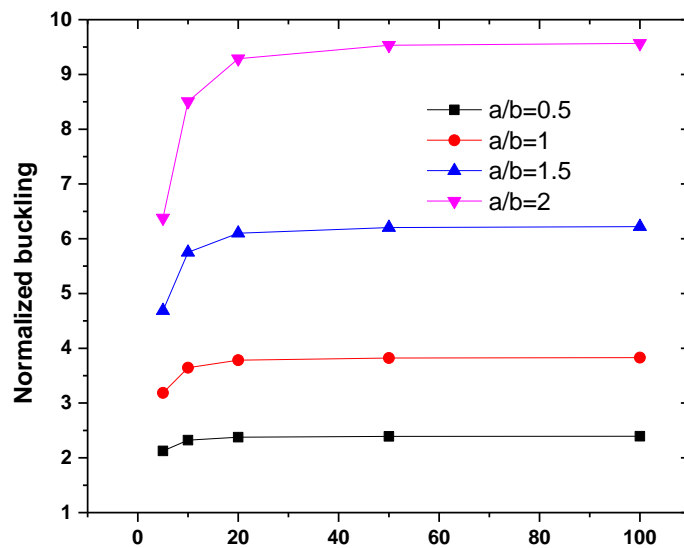


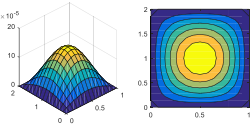
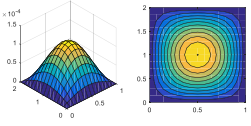
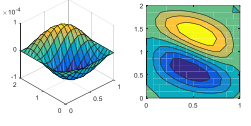
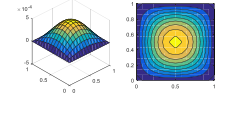
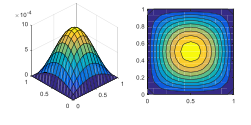
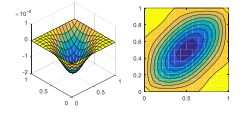
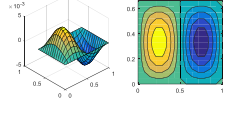
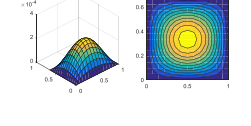
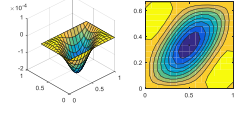
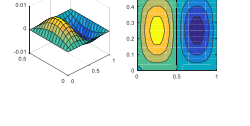
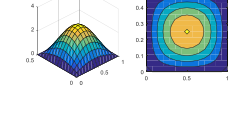
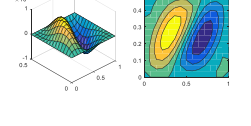
Fig 4: The effect of span to thickness ratio with aspect ratio on normalized buckling  $\bar{N}_{cr} = N_{cr} a^2 / E_m h^3$  of FGM plate under biaxial loading.

4.3.2 Effect of in-plane loading with aspect ratio.

Table 6 represents the effect of aspect ratio on normalized buckling  $\bar{N}_{cr} = N_{cr} / E_m h^3$  of FGM plate (a/h=10,

$n=1, g=11$ ) under uniaxial, biaxial and pure shear loading. It is observed that by increasing the aspect ratio, normalized buckling increases for all the loading. Pure shear loading predicts maximum normalized buckling as compared to another loading.

**Table 6 Normalized buckling and counters shape of FGM plate under various types of loading**

a/b	Uniaxial loading	Biaxial loading	Pure shear loading
0.5	 <p>3.719</p>	 <p>2.97</p>	 <p>14.44</p>
1	 <p>9.36</p>	 <p>4.68</p>	 <p>19.6584</p>
1.5	 <p>20.876</p>	 <p>7.39</p>	 <p>30.882</p>
2	 <p>33.03</p>	 <p>10.96</p>	 <p>44.48</p>

### 5 CONCLUSIONS

Thirteen RBFs have been compared for buckling behaviour of rectangular FGM plate obtained from five variables higher-order shear deformation theory. The benchmark results from the literature verify the effectiveness of the modified RBFs. The computational speed of RBFs  $g_2, g_{10}, g_{11}, g_{12}$ , and  $g_{13}$  is reasonable as compared to other RBFs taken here. It also concluded that modified radial distances in RBFs are helpful in predicting the buckling response of rectangular plates with different aspect ratios, which was not obtained without changing the radial distance of RBFs. It is observed that normalized buckling load decreases with an increase in  $a/b$  and grading index; however, it increases as the span to thickness ratio increases.

### REFERENCES

[1] R. L. Hardy, "Multiquadric equations of topography and other irregular surfaces," *Journal of geophysical research*, vol. 76, no. 8, pp. 1905-1915, 1971.

[2] E. J. Kansa, "Multiquadrics—A scattered data approximation scheme with applications to computational fluid-dynamics—I surface approximations and partial derivative estimates," *Computers & Mathematics with applications*, vol. 19, no. 8-9, pp. 127-145, 1990.

[3] E. J. Kansa, "Multiquadrics—A scattered data approximation scheme with applications to computational fluid-dynamics—II solutions to parabolic, hyperbolic and elliptic partial differential equations," *Computers & mathematics with applications*, vol. 19, no. 8-9, pp. 147-161, 1990.

- [4] V. Bayona, M. Moscoso, and M. Kindelan, "Optimal variable shape parameter for multiquadric based RBF-FD method," *Journal of Computational Physics*, vol. 231, no. 6, pp. 2466-2481, 2012.
- [5] C.-S. Huang, C.-F. Lee, and A.-D. Cheng, "Error estimate, optimal shape factor, and high precision computation of multiquadric collocation method," *Engineering Analysis with Boundary Elements*, vol. 31, no. 7, pp. 614-623, 2007.
- [6] C.-S. Huang, H.-D. Yen, and A.-D. Cheng, "On the increasingly flat radial basis function and optimal shape parameter for the solution of elliptic PDEs," *Engineering analysis with boundary elements*, vol. 34, no. 9, pp. 802-809, 2010.
- [7] L. Iurlaro, M. Gherlone, and M. Di Sciuva, "Energy based approach for shape parameter selection in radial basis functions collocation method," *Composite Structures*, vol. 107, pp. 70-78, 2014.
- [8] S. Rippa, "An algorithm for selecting a good value for the parameter  $c$  in radial basis function interpolation," *Advances in Computational Mathematics*, vol. 11, no. 2, pp. 193-210, 1999.
- [9] G. E. Fasshauer, "Solving partial differential equations by collocation with radial basis functions," in *Proceedings of Chamonix*, 1996, vol. 1997: Citeseer, pp. 1-8.
- [10] H. Wendland, "Meshless Galerkin methods using radial basis functions," *Mathematics of computation*, vol. 68, no. 228, pp. 1521-1531, 1999.
- [11] B. V. Farahani, J. Berardo, J. Belinha, A. Ferreira, P. J. Tavares, and P. Moreira, "On the optimal shape parameters of distinct versions of RBF meshless methods for the bending analysis of plates," *Engineering Analysis with Boundary Elements*, vol. 84, pp. 77-86, 2017.
- [12] A. Ferreira, "A formulation of the multiquadric radial basis function method for the analysis of laminated composite plates," *Composite structures*, vol. 59, no. 3, pp. 385-392, 2003.
- [13] A. Ferreira, E. Carrera, M. Cinefra, C. Roque, and O. Polit, "Analysis of laminated shells by a sinusoidal shear deformation theory and radial basis functions collocation, accounting for through-the-thickness deformations," *Composites Part B: Engineering*, vol. 42, no. 5, pp. 1276-1284, 2011.
- [14] A. Ferreira and G. Fasshauer, "Computation of natural frequencies of shear deformable beams and plates by an RBF-pseudospectral method," *Computer Methods in Applied Mechanics and Engineering*, vol. 196, no. 1-3, pp. 134-146, 2006.
- [15] A. Ferreira, G. Fasshauer, R. Batra, and J. Rodrigues, "Static deformations and vibration analysis of composite and sandwich plates using a layerwise theory and RBF-PS discretizations with optimal shape parameter," *Composite Structures*, vol. 86, no. 4, pp. 328-343, 2008.
- [16] A. Ferreira, C. Roque, and R. Jorge, "Free vibration analysis of symmetric laminated composite plates by FSDT and radial basis functions," *Computer Methods in Applied Mechanics and Engineering*, vol. 194, no. 39-41, pp. 4265-4278, 2005.
- [17] A. Ferreira, C. Roque, R. Jorge, and E. Kansa, "Static deformations and vibration analysis of composite and sandwich plates using a layerwise theory and multiquadrics discretizations," *Engineering Analysis with Boundary Elements*, vol. 29, no. 12, pp. 1104-1114, 2005.
- [18] A. Ferreira, C. Roque, and P. Martins, "Analysis of composite plates using higher-order shear deformation theory and a finite point formulation based on the multiquadric radial basis function method," *Composites Part B: Engineering*, vol. 34, no. 7, pp. 627-636, 2003.
- [19] A. Ferreira, C. Roque, A. Neves, R. Jorge, C. Soares, and K. M. Liew, "Buckling and vibration analysis of isotropic and laminated plates by radial basis functions," *Composites Part B: Engineering*, vol. 42, no. 3, pp. 592-606, 2011.
- [20] A. Ferreira, C. Roque, A. Neves, R. Jorge, C. M. Soares, and J. Reddy, "Buckling analysis of isotropic and laminated plates by radial basis functions according to a higher-order shear deformation theory," *Thin-Walled Structures*, vol. 49, no. 7, pp. 804-811, 2011.
- [21] M. Jakomin, F. Kosel, and T. Kosel, "Thin double curved shallow bimetallic shell of translation in a homogenous temperature field by non-linear theory," *Thin-walled structures*, vol. 48, no. 3, pp. 243-259, 2010.
- [22] S. Xiang, Z.-y. Bi, S.-x. Jiang, Y.-x. Jin, and M.-s. Yang, "Thin plate spline radial basis function for the free vibration analysis of laminated composite shells," *Composite Structures*, vol. 93, no. 2, pp. 611-615, 2011.
- [23] S. Xiang, S.-x. Jiang, Z.-y. Bi, Y.-x. Jin, and M.-s. Yang, "A  $n$ th-order meshless generalization of Reddy's third-order shear deformation theory for the free vibration on laminated composite plates," *Composite Structures*, vol. 93, no. 2, pp. 299-307, 2011.
- [24] S. Xiang, H. Shi, K.-m. Wang, Y.-t. Ai, and Y.-d. Sha, "Thin plate spline radial basis functions for vibration analysis of clamped laminated composite plates," *European Journal of Mechanics-A/Solids*, vol. 29, no. 5, pp. 844-850, 2010.

- [25] S. Xiang and K.-m. Wang, "Free vibration analysis of symmetric laminated composite plates by trigonometric shear deformation theory and inverse multiquadric RBF," *Thin-Walled Structures*, vol. 47, no. 3, pp. 304-310, 2009.
- [26] J. Rodrigues, C. Roque, A. Ferreira, E. Carrera, and M. Cinefra, "Radial basis functions–finite differences collocation and a Unified Formulation for bending, vibration and buckling analysis of laminated plates, according to Murakami's zig-zag theory," *Composite Structures*, vol. 93, no. 7, pp. 1613-1620, 2011.
- [27] C. Roque, D. Cunha, C. Shu, and A. Ferreira, "A local radial basis functions—Finite differences technique for the analysis of composite plates," *Engineering Analysis with Boundary Elements*, vol. 35, no. 3, pp. 363-374, 2011.
- [28] R. B. Prasad, J. Singh, and K. K. Shukla, "Application of radial basis function-based meshless method for torsional analysis of elliptical and bone shaped-irregular sections," *Proceedings of the Institution of Mechanical Engineers, Part L: Journal of Materials: Design and Applications*, vol. 236, no. 3, pp. 611-632, 2022.
- [29] J. Singh and K. Shukla, "Nonlinear flexural analysis of functionally graded plates under different loadings using RBF based meshless method," *Engineering Analysis with Boundary Elements*, vol. 36, no. 12, pp. 1819-1827, 2012.
- [30] J. Singh and K. Shukla, "Nonlinear flexural analysis of laminated composite plates using RBF based meshless method," *Composite Structures*, vol. 94, no. 5, pp. 1714-1720, 2012.
- [31] J. Singh, S. Singh, and K. Shukla, "RBF-based meshless method for free vibration analysis of laminated composite plates," *International Journal of Mechanical and Mechatronics Engineering*, vol. 5, no. 7, pp. 1290-1295, 2011.
- [32] J. Singh, S. Singh, and K. Shukla, "Meshless analysis of laminated composite and sandwich plates subjected to various types of loads," *International Journal for Computational Methods in Engineering Science and Mechanics*, vol. 15, no. 2, pp. 158-171, 2014.
- [33] S. Singh, J. Singh, and K. Shukla, "Buckling of laminated composite plates subjected to mechanical and thermal loads using meshless collocations," *Journal of Mechanical Science and Technology*, vol. 27, no. 2, pp. 327-336, 2013.
- [34] S. Singh, J. Singh, and K. K. Shula, "Buckling of laminated composite and sandwich plates using radial basis function collocations," *International Journal of Structural Stability and Dynamics*, vol. 15, no. 01, p. 1540002, 2015.
- [35] M. K. Solanki, R. Kumar, and J. Singh, "Flexure analysis of laminated plates using multiquadratic RBF based meshfree method," *International Journal of Computational Methods*, vol. 15, no. 06, p. 1850049, 2018.
- [36] M. K. Solanki, S. K. Mishra, K. Shukla, and J. Singh, "Nonlinear free vibration of laminated composite and sandwich plates using multiquadric collocations," *Materials Today: Proceedings*, vol. 2, no. 4-5, pp. 3049-3055, 2015.
- [37] M. K. Solanki, S. K. Mishra, and J. Singh, "Meshfree approach for linear and nonlinear analysis of sandwich plates: A critical review of twenty plate theories," *Engineering Analysis with Boundary Elements*, vol. 69, pp. 93-103, 2016.
- [38] P. C. Vishwakarma, J. Damania, and J. Singh, "Improving Vibration analysis of laminated composite plate by using WU-C2 RBF based Meshfree Method," in *IOP Conference Series: Materials Science and Engineering*, 2018, vol. 404, no. 1: IOP Publishing, p. 012036.
- [39] A. Kumar, R. Kumar, J. Damania, and J. Singh, "Buckling Analysis of FGM Plates by thin plate spline RBF based Meshfree Approach," in *IOP Conference Series: Materials Science and Engineering*, 2018, vol. 404, no. 1: IOP Publishing, p. 012037.
- [40] R. Kumar, M. Bajaj, J. Singh, and K. K. Shukla, "New HSDT for free vibration analysis of elastically supported porous bidirectional functionally graded sandwich plate using collocation method," *Proceedings of the Institution of Mechanical Engineers, Part C: Journal of Mechanical Engineering Science*, p. 09544062221090075, 2022.
- [41] R. Kumar, A. Lal, B. Singh, and J. Singh, "New transverse shear deformation theory for bending analysis of FGM plate under patch load," *Composite Structures*, vol. 208, pp. 91-100, 2019.
- [42] R. Kumar, A. Lal, B. Singh, and J. Singh, "Meshfree approach on buckling and free vibration analysis of porous FGM plate with proposed IHSDT resting on the foundation," *Curved and Layered Structures*, vol. 6, no. 1, pp. 192-211, 2019.
- [43] R. Kumar, A. Lal, B. Singh, and J. Singh, "Non-linear analysis of porous elastically supported FGM plate under various loading," *Composite Structures*, vol. 233, p. 111721, 2020.
- [44] R. Kumar, A. Lal, B. N. Singh, and J. Singh, "Numerical simulation of the thermomechanical buckling analysis of bidirectional porous functionally graded plate using collocation meshfree method," *Proceedings*

- of the Institution of Mechanical Engineers, Part L: Journal of Materials: Design and Applications, vol. 236, no. 4, pp. 787-807, 2022.
- [45] R. Kumar, A. Lal, and J. Singh, "Meshfree approach for the vibration analysis of FGM plates using two shear displacement model," in *Proceedings of the third Indian conference on applied mechanics*, 2017.
- [46] R. Kumar, B. Singh, and J. Singh, "Geometrically nonlinear analysis for flexure response of FGM plate under patch load," *Mechanics Based Design of Structures and Machines*, pp. 1-25, 2022.
- [47] R. Kumar and J. Singh, "Assessment of higher order transverse shear deformation theories for modeling and buckling analysis of FGM plates using RBF based meshless approach," *Multidiscipline Modeling in Materials and Structures*, 2018.
- [48] A. Neves, A. Ferreira, E. Carrera, M. Cinefra, R. Jorge, and C. Soares, "Buckling analysis of sandwich plates with functionally graded skins using a new quasi-3D hyperbolic sine shear deformation theory and collocation with radial basis functions," *ZAMM-Journal of Applied Mathematics and Mechanics/Zeitschrift für Angewandte Mathematik und Mechanik*, vol. 92, no. 9, pp. 749-766, 2012.
- [49] A. Neves et al., "A quasi-3D hyperbolic shear deformation theory for the static and free vibration analysis of functionally graded plates," *Composite Structures*, vol. 94, no. 5, pp. 1814-1825, 2012.
- [50] A. Neves et al., "Static, free vibration and buckling analysis of isotropic and sandwich functionally graded plates using a quasi-3D higher-order shear deformation theory and a meshless technique," *Composites Part B: Engineering*, vol. 44, no. 1, pp. 657-674, 2013.
- [51] D. Maturi, A. Ferreira, A. Zenkour, and D. Mashat, "Analysis of sandwich plates with a new layerwise formulation," *Composites Part B: Engineering*, vol. 56, pp. 484-489, 2014.
- [52] C. H. Thai, V. N. Do, and H. Nguyen-Xuan, "An improved Moving Kriging-based meshfree method for static, dynamic and buckling analyses of functionally graded isotropic and sandwich plates," *Engineering Analysis with Boundary Elements*, vol. 64, pp. 122-136, 2016.
- [53] T. Bui, M. Nguyen, and C. Zhang, "Buckling analysis of Reissner–Mindlin plates subjected to in-plane edge loads using a shear-locking-free and meshfree method," *Engineering analysis with boundary elements*, vol. 35, no. 9, pp. 1038-1053, 2011.
- [54] J. Rodrigues, C. Roque, A. Ferreira, M. Cinefra, and E. Carrera, "Radial basis functions-differential quadrature collocation and a unified formulation for bending, vibration and buckling analysis of laminated plates, according to Murakami's Zig-Zag theory," *Computers & structures*, vol. 90, pp. 107-115, 2012.
- [55] F. Chu, J. He, L. Wang, and Z. Zhong, "Buckling analysis of functionally graded thin plate with in-plane material inhomogeneity," *Engineering Analysis with Boundary Elements*, vol. 65, pp. 112-125, 2016.
- [56] A. Farajpour, M. Danesh, and M. Mohammadi, "Buckling analysis of variable thickness nanoplates using nonlocal continuum mechanics," *Physica E: Low-dimensional Systems and Nanostructures*, vol. 44, no. 3, pp. 719-727, 2011.
- [57] A. Farajpour, M. Mohammadi, A. Shahidi, and M. Mahzoon, "Axisymmetric buckling of the circular graphene sheets with the nonlocal continuum plate model," *Physica E: Low-dimensional Systems and Nanostructures*, vol. 43, no. 10, pp. 1820-1825, 2011.
- [58] A. Farajpour, A. Rastgoo, and M. Mohammadi, "Vibration, buckling and smart control of microtubules using piezoelectric nanoshells under electric voltage in thermal environment," *Physica B: Condensed Matter*, vol. 509, pp. 100-114, 2017.
- [59] A. Farajpour, A. Shahidi, M. Mohammadi, and M. Mahzoon, "Buckling of orthotropic micro/nanoscale plates under linearly varying in-plane load via nonlocal continuum mechanics," *Composite Structures*, vol. 94, no. 5, pp. 1605-1615, 2012.
- [60] A. Hadi, M. Z. Nejad, A. Rastgoo, and M. Hosseini, "Buckling analysis of FGM Euler-Bernoulli nano-beams with 3D-varying properties based on consistent couple-stress theory," *Steel and Composite Structures, An International Journal*, vol. 26, no. 6, pp. 663-672, 2018.
- [61] M. Mohammadi, A. Farajpour, A. Moradi, and M. Ghayour, "Shear buckling of orthotropic rectangular graphene sheet embedded in an elastic medium in thermal environment," *Composites Part B: Engineering*, vol. 56, pp. 629-637, 2014.
- [62] M. Z. Nejad, A. Hadi, and A. Rastgoo, "Buckling analysis of arbitrary two-directional functionally graded Euler–Bernoulli nano-beams based on nonlocal elasticity theory," *International Journal of Engineering Science*, vol. 103, pp. 1-10, 2016.
- [63] K. Liew, J. Wang, T. Ng, and M. Tan, "Free vibration and buckling analyses of shear-deformable plates based on FSDT meshfree method," *Journal of Sound and Vibration*, vol. 276, no. 3-5, pp. 997-1017, 2004.
- [64] L. Zhang, P. Zhu, and K. Liew, "Thermal buckling of functionally graded plates using a local Kriging meshless method," *Composite Structures*, vol. 108, pp. 472-492, 2014.

- [65] P. Tan, N. Nguyen-Thanh, T. Rabczuk, and K. Zhou, "Static, dynamic and buckling analyses of 3D FGM plates and shells via an isogeometric-meshfree coupling approach," *Composite Structures*, vol. 198, pp. 35-50, 2018.
- [66] A. Zarei and A. Khosravifard, "A meshfree method for static and buckling analysis of shear deformable composite laminates considering continuity of interlaminar transverse shearing stresses," *Composite Structures*, vol. 209, pp. 206-218, 2019.
- [67] H. Asemi, S. Asemi, A. Farajpour, and M. Mohammadi, "Nanoscale mass detection based on vibrating piezoelectric ultrathin films under thermo-electro-mechanical loads," *Physica E: Low-dimensional Systems and Nanostructures*, vol. 68, pp. 112-122, 2015.
- [68] S. Asemi, A. Farajpour, H. Asemi, and M. Mohammadi, "Influence of initial stress on the vibration of double-piezoelectric-nanoplate systems with various boundary conditions using DQM," *Physica E: Low-dimensional Systems and Nanostructures*, vol. 63, pp. 169-179, 2014.
- [69] S. Asemi, A. Farajpour, and M. Mohammadi, "Nonlinear vibration analysis of piezoelectric nanoelectromechanical resonators based on nonlocal elasticity theory," *Composite Structures*, vol. 116, pp. 703-712, 2014.
- [70] A. Barati, A. Hadi, M. Z. Nejad, and R. Noroozi, "On vibration of bi-directional functionally graded nanobeams under magnetic field," *Mechanics Based Design of Structures and Machines*, vol. 50, no. 2, pp. 468-485, 2022.
- [71] M. Danesh, A. Farajpour, and M. Mohammadi, "Axial vibration analysis of a tapered nanorod based on nonlocal elasticity theory and differential quadrature method," *Mechanics Research Communications*, vol. 39, no. 1, pp. 23-27, 2012.
- [72] A. Farajpour, M. H. Yazdi, A. Rastgoo, M. Loghmani, and M. Mohammadi, "Nonlocal nonlinear plate model for large amplitude vibration of magneto-electro-elastic nanoplates," *Composite Structures*, vol. 140, pp. 323-336, 2016.
- [73] M. R. Farajpour, A. Rastgoo, A. Farajpour, and M. Mohammadi, "Vibration of piezoelectric nanofilm-based electromechanical sensors via higher-order non-local strain gradient theory," *Micro & Nano Letters*, vol. 11, no. 6, pp. 302-307, 2016.
- [74] A. Hadi, M. Z. Nejad, and M. Hosseini, "Vibrations of three-dimensionally graded nanobeams," *International Journal of Engineering Science*, vol. 128, pp. 12-23, 2018.
- [75] A. Hadi, A. Rastgoo, A. Daneshmehr, and F. Ehsani, "Stress and strain analysis of functionally graded rectangular plate with exponentially varying properties," *Indian Journal of Materials Science*, vol. 2013, 2013.
- [76] M. Mohammadi, A. Farajpour, M. Goodarzi, and F. Dinari, "Thermo-mechanical vibration analysis of annular and circular graphene sheet embedded in an elastic medium," *Latin American Journal of Solids and Structures*, vol. 11, pp. 659-682, 2014.
- [77] M. Mohammadi, A. Farajpour, M. Goodarzi, and H. Mohammadi, "Temperature Effect on Vibration Analysis of Annular Graphene Sheet Embedded on Visco-Pasternak Foundati," *Journal of Solid Mechanics*, vol. 5, no. 3, pp. 305-323, 2013. [Online]. Available: [http://jsm.iau-arak.ac.ir/article\\_514574\\_947d5d6914c8c336b9a9ba095eeac2f6.pdf](http://jsm.iau-arak.ac.ir/article_514574_947d5d6914c8c336b9a9ba095eeac2f6.pdf).
- [78] M. Mohammadi, M. Ghayour, and A. Farajpour, "Analysis of free vibration sector plate based on elastic medium by using new version of differential quadrature method," *Journal of Simulation and Analysis of Novel Technologies in Mechanical Engineering*, vol. 3, no. 2, pp. 47-56, 2010.
- [79] M. Mohammadi, M. Ghayour, and A. Farajpour, "Free transverse vibration analysis of circular and annular graphene sheets with various boundary conditions using the nonlocal continuum plate model," *Composites Part B: Engineering*, vol. 45, no. 1, pp. 32-42, 2013.
- [80] M. Mohammadi, M. Goodarzi, M. Ghayour, and A. Farajpour, "Influence of in-plane pre-load on the vibration frequency of circular graphene sheet via nonlocal continuum theory," *Composites Part B: Engineering*, vol. 51, pp. 121-129, 2013.
- [81] M. Mohammadi, M. Hosseini, M. Shishesaz, A. Hadi, and A. Rastgoo, "Primary and secondary resonance analysis of porous functionally graded nanobeam resting on a nonlinear foundation subjected to mechanical and electrical loads," *European Journal of Mechanics-A/Solids*, vol. 77, p. 103793, 2019.
- [82] M. Mohammadi, A. Moradi, M. Ghayour, and A. Farajpour, "Exact solution for thermo-mechanical vibration of orthotropic mono-layer graphene sheet embedded in an elastic medium," *Latin American Journal of Solids and Structures*, vol. 11, pp. 437-458, 2014.
- [83] M. Mohammadi and A. Rastgoo, "Nonlinear vibration analysis of the viscoelastic composite nanoplate with three directionally imperfect porous FG core," *Structural Engineering and Mechanics, An Int'l Journal*, vol. 69, no. 2, pp. 131-143, 2019.

- [84] M. Mohammadi and A. Rastgoo, "Primary and secondary resonance analysis of FG/lipid nanoplate with considering porosity distribution based on a nonlinear elastic medium," *Mechanics of Advanced Materials and Structures*, vol. 27, no. 20, pp. 1709-1730, 2020/10/15 2020, doi: 10.1080/15376494.2018.1525453.
- [85] M. Mohammadi, M. Safarabadi, A. Rastgoo, and A. Farajpour, "Hygro-mechanical vibration analysis of a rotating viscoelastic nanobeam embedded in a visco-Pasternak elastic medium and in a nonlinear thermal environment," *Acta Mechanica*, vol. 227, no. 8, pp. 2207-2232, 2016.
- [86] H. Moosavi, M. Mohammadi, A. Farajpour, and S. Shahidi, "Vibration analysis of nanorings using nonlocal continuum mechanics and shear deformable ring theory," *Physica E: Low-dimensional Systems and Nanostructures*, vol. 44, no. 1, pp. 135-140, 2011.
- [87] R. Noroozi, A. Barati, A. Kazemi, S. Norouzi, and A. Hadi, "Torsional vibration analysis of bi-directional FG nano-cone with arbitrary cross-section based on nonlocal strain gradient elasticity," *Advances in nano research*, vol. 8, no. 1, pp. 13-24, 2020.
- [88] N. GHAYOUR, A. SEDAGHAT, and M. MOHAMMADI, "WAVE PROPAGATION APPROACH TO FLUID FILLED SUBMERGED VISCO-ELASTIC FINITE CYLINDRICAL SHELLS," *JOURNAL OF AEROSPACE SCIENCE AND TECHNOLOGY (JAST)*, vol. 8, no. 1, pp. -, 2011. [Online]. Available: <https://www.sid.ir/en/Journal/ViewPaper.aspx?ID=254379>.
- [89] H. Moosavi, M. Mohammadi, A. Farajpour, and S. H. Shahidi, "Vibration analysis of nanorings using nonlocal continuum mechanics and shear deformable ring theory," *Physica E: Low-dimensional Systems and Nanostructures*, vol. 44, no. 1, pp. 135-140, 2011/10/01/ 2011, doi: <https://doi.org/10.1016/j.physe.2011.08.002>.
- [90] M. MOHAMMADI, M. GOODARZI, M. GHAYOUR, and S. ALIVAND, "SMALL SCALE EFFECT ON THE VIBRATION OF ORTHOTROPIC PLATES EMBEDDED IN AN ELASTIC MEDIUM AND UNDER BIAxIAL IN-PLANE PRE-LOAD VIA NONLOCAL ELASTICITY THEORY," *JOURNAL OF SOLID MECHANICS*, vol. 4, no. 2, pp. -, 2012. [Online]. Available: <https://www.sid.ir/en/Journal/ViewPaper.aspx?ID=303684>.
- [91] M. Mohammadi, M. Goodarzi, M. Ghayour, and S. Alivand, "Small scale effect on the vibration of orthotropic plates embedded in an elastic medium and under biaxial in-plane pre-load via nonlocal elasticity theory," 2012.
- [92] M. Mohammadi, A. Farajpour, M. Goodarzi, and R. Heydarshenas, "Levy Type Solution for Nonlocal Thermo-Mechanical Vibration of Orthotropic Mono-Layer Graphene Sheet Embedded in an Elastic Medium," *Journal of Solid Mechanics*, vol. 5, no. 2, pp. 116-132, 2013. [Online]. Available: [http://jsm.iauarak.ac.ir/article\\_514544\\_042ba549d411678ff6d41c27993d17c.pdf](http://jsm.iauarak.ac.ir/article_514544_042ba549d411678ff6d41c27993d17c.pdf).
- [93] M. Mohammadi, A. Farajpour, M. Goodarzi, and H. Shehni nezhad pour, "Numerical study of the effect of shear in-plane load on the vibration analysis of graphene sheet embedded in an elastic medium," *Computational Materials Science*, vol. 82, pp. 510-520, 2014/02/01/ 2014, doi: <https://doi.org/10.1016/j.commatsci.2013.10.022>.
- [94] A. Farajpour, A. Rastgoo, and M. Mohammadi, "Surface effects on the mechanical characteristics of microtubule networks in living cells," *Mechanics Research Communications*, vol. 57, pp. 18-26, 2014/04/01/ 2014, doi: <https://doi.org/10.1016/j.mechrescom.2014.01.005>.
- [95] M. GOODARZI, M. MOHAMMADI, A. FARAJPOUR, and M. KHOORAN, "INVESTIGATION OF THE EFFECT OF PRE-STRESSED ON VIBRATION FREQUENCY OF RECTANGULAR NANOPATE BASED ON A VISCO-PASTERNAK FOUNDATION," *JOURNAL OF SOLID MECHANICS*, vol. 6, no. 1, pp. -, 2014. [Online]. Available: <https://www.sid.ir/en/Journal/ViewPaper.aspx?ID=376801>.
- [96] S. R. Asemi, M. Mohammadi, and A. Farajpour, "A study on the nonlinear stability of orthotropic single-layered graphene sheet based on nonlocal elasticity theory," *Latin American Journal of Solids and Structures*, vol. 11, no. 9, pp. 1515-1540, 2014.
- [97] M. Mohammadi, A. Moradi, M. Ghayour, and A. Farajpour, "Exact solution for thermo-mechanical vibration of orthotropic mono-layer graphene sheet embedded in an elastic medium," *Latin American Journal of Solids and Structures*, vol. 11, no. 3, pp. 437-458, 2014.
- [98] M. Mohammadi, A. Farajpour, and M. Goodarzi, "Numerical study of the effect of shear in-plane load on the vibration analysis of graphene sheet embedded in an elastic medium," *Computational Materials Science*, vol. 82, pp. 510-520, 2014.
- [99] M. Safarabadi, M. Mohammadi, A. Farajpour, and M. Goodarzi, "Effect of surface energy on the vibration analysis of rotating nanobeam," 2015.
- [100] M. Goodarzi, M. Mohammadi, M. Khooran, and F. Saadi, "Thermo-Mechanical Vibration Analysis of FG Circular and Annular Nanoplate Based on the Visco-Pasternak Foundation," *Journal of Solid Mechanics*,

- vol. 8, no. 4, pp. 788-805, 2016. [Online]. Available: [http://jsm.iau-arak.ac.ir/article\\_527024\\_c73ec8e3fa8e3b28dd54dbd53891d503.pdf](http://jsm.iau-arak.ac.ir/article_527024_c73ec8e3fa8e3b28dd54dbd53891d503.pdf).
- [101] M. Baghani, M. Mohammadi, and A. Farajpour, "Dynamic and Stability Analysis of the Rotating Nanobeam in a Nonuniform Magnetic Field Considering the Surface Energy," *International Journal of Applied Mechanics*, vol. 08, no. 04, p. 1650048, 2016, doi: 10.1142/s1758825116500484.
- [102] M. R. Farajpour, A. Rastgoo, A. Farajpour, and M. Mohammadi, "Vibration of piezoelectric nanofilm-based electromechanical sensors via higher-order non-local strain gradient theory," *Micro & Nano Letters*, vol. 11, no. 6, pp. 302-307, 2016.
- [103] A. Farajpour, M. Yazdi, A. Rastgoo, and M. Mohammadi, "A higher-order nonlocal strain gradient plate model for buckling of orthotropic nanoplates in thermal environment," *Acta Mechanica*, vol. 227, no. 7, pp. 1849-1867, 2016.
- [104] M. Mohammadi, M. Hosseini, M. Shishesaz, A. Hadi, and A. Rastgoo, "Primary and secondary resonance analysis of porous functionally graded nanobeam resting on a nonlinear foundation subjected to mechanical and electrical loads," *European Journal of Mechanics - A/Solids*, vol. 77, p. 103793, 2019/09/01/ 2019, doi: <https://doi.org/10.1016/j.euromechsol.2019.05.008>.
- [105] M. Mohammadi, A. Farajpour, A. Moradi, and M. Hosseini, "Vibration analysis of the rotating multilayer piezoelectric Timoshenko nanobeam," *Engineering Analysis with Boundary Elements*, vol. 145, pp. 117-131, 2022/12/01/ 2022, doi: <https://doi.org/10.1016/j.enganabound.2022.09.008>.
- [106] M. Hosseini, M. Shishesaz, K. N. Tahan, and A. Hadi, "Stress analysis of rotating nano-disks of variable thickness made of functionally graded materials," *International Journal of Engineering Science*, vol. 109, pp. 29-53, 2016.
- [107] M. Z. Nejad, A. Hadi, A. Omidvari, and A. Rastgoo, "Bending analysis of bi-directional functionally graded Euler-Bernoulli nano-beams using integral form of Eringen's non-local elasticity theory," *Structural engineering and mechanics: An international journal*, vol. 67, no. 4, pp. 417-425, 2018.
- [108] M. M. Khoram, M. Hosseini, A. Hadi, and M. Shishesaz, "Bending analysis of bidirectional FGM Timoshenko nanobeam subjected to mechanical and magnetic forces and resting on Winkler–Pasternak foundation," *International Journal of Applied Mechanics*, vol. 12, no. 08, p. 2050093, 2020.
- [109] V. N. Van Do, M. T. Tran, and C.-H. Lee, "Nonlinear thermal buckling analyses of functionally graded plates by a mesh-free radial point interpolation method," *Engineering Analysis with Boundary Elements*, vol. 87, pp. 153-164, 2018.
- [110] S. R. Asemi, M. Mohammadi, and A. Farajpour, "A study on the nonlinear stability of orthotropic single-layered graphene sheet based on nonlocal elasticity theory," *Latin American Journal of Solids and Structures*, vol. 11, pp. 1541-1546, 2014.
- [111] A. Hadi, A. Daneshmehr, S. N. Mehriani, M. Hosseini, and F. Ehsani, "Elastic analysis of functionally graded Timoshenko beam subjected to transverse loading," *Technical Journal of Engineering and Applied Sciences*, vol. 3, no. 13, pp. 1246-1254, 2013.
- [112] T.-K. Nguyen, "A higher-order hyperbolic shear deformation plate model for analysis of functionally graded materials," *International Journal of Mechanics and Materials in Design*, vol. 11, no. 2, pp. 203-219, 2015.
- [113] M. Sekkal, B. Fahsi, A. Tounsi, and S. Mahmoud, "A new quasi-3D HSDT for buckling and vibration of FG plate," *Structural engineering and mechanics: An international journal*, vol. 64, no. 6, pp. 737-749, 2017.
- [114] T. Teo and K. Liew, "A differential quadrature procedure for three-dimensional buckling analysis of rectangular plates," *International journal of solids and structures*, vol. 36, no. 8, pp. 1149-1168, 1999.